

# Cinobufagin disrupts the stability of lipid rafts by inhibiting the expression of caveolin-1 to promote non-small cell lung cancer cell apoptosis

Zhongqing Xu, Jinwei Li, Shuyu Fang, Mingzhu Lian, Changxiao Zhang, Jiahuan Lu, Kai Sheng

Department of Gerontology, Tongren Hospital, Shanghai Jiao Tong University School of Medicine, Shanghai, China

**Submitted:** 2 August 2023; **Accepted:** 27 October 2023

**Online publication:** 28 June 2024

Arch Med Sci 2024; 20 (3): 887–908

DOI: <https://doi.org/10.5114/aoms/174578>

Copyright © 2024 Termedia & Banach

## Corresponding authors:

Jiahuan Lu

Kai Sheng

Department of Gerontology

Tongren Hospital

Shanghai Jiao Tong

University School

of Medicine

1111 Xianxia Road

Shanghai 200336, China

E-mail: LJH2559@

shtrhospital.com;

SK1800@shtrhospital.com

## Abstract

**Introduction:** The study was designed to explore how cinobufagin (CB) regulates the development of non-small cell lung cancer (NSCLC) cells through lipid rafts.

**Material and methods:** The effects of CB at gradient concentrations (0, 0.5, 1 and 2  $\mu\text{M}$ ) on NSCLC cell viability, apoptosis, reactive oxygen species (ROS) level, phosphorylation of Akt, and apoptosis- and lipid raft-related protein expression were assessed by MTT assay, flow cytometry and Western blot. Cholesterol and sphingomyelin were labeled with BODIPY to evaluate the effect of CB (2  $\mu\text{M}$ ) on them. Sucrose density gradient centrifugation was used to extract lipid rafts. The effect of CB on the expression and distribution of caveolin-1 was determined by immunofluorescence, quantitative reverse transcription polymerase chain reaction and Western blot. After overexpression of caveolin-1, the above experiments were performed again to observe whether the regulatory effect of CB was reversed.

**Results:** CB inhibited NSCLC cell viability while promoting apoptosis and ROS level. CB redistributed the lipid content on the membrane surface and reduced the content of caveolin-1 in the cell membrane. In addition, CB repressed the activation of AKT. However, caveolin-1 overexpression reversed the effects of CB on apoptosis, AKT activation and lipid raft.

**Conclusions:** CB regulates the activity of Akt in lipid rafts by inhibiting caveolin-1 expression to promote NSCLC cell apoptosis.

**Key words:** non-small cell lung cancer, cinobufagin, lipid rafts, caveolin-1.

## Introduction

Among the histological types of lung cancer, non-small cell lung cancer (NSCLC) accounts for about 85%, with one-third of initially diagnosed patients already at stage III [1]. Although the treatment of lung cancer has advanced by leaps and bounds in recent years, the survival rate of patients has not markedly improved [2]. Therefore, seeking effective novel treatment strategies is crucial to prolong the survival time of patients.

In recent years, traditional Chinese medicine has attracted the attention of scientists by virtue of its advantages such as multiple targets and small side effects [3, 4]. ChanSu, a precious Chinese medicine, is made from the substance secreted by *Bufo gargarizans* Cantor or *Bufo melanostictus* Schneider [5]. Cinobufagin (CB) is the main ingredient of ChanSu, with many functions, including anti-tumor activity, immune

regulation, pain relief, heart strengthening, etc. [6]. Notably, CB has anti-cancer effects on osteosarcoma [7], nasopharyngeal carcinoma [8], melanoma [9], colorectal cancer [10] and lung cancer [11]. However, there still exists a knowledge gap in the regulatory mechanism of CB in lung cancer. Lipid rafts are membrane microdomains rich in cholesterol and sphingomyelin with a variety of special proteins, including caveolin, flotillin (FLOT), glycosylphosphatidylinositol-anchored protein and palmitoyl protein [12]. They have been perceived as a platform for interactions between various cell surface receptors and signal molecules [13]. Jeon *et al.* proposed that lipid rafts can affect the migration of NSCLC cells [14]. Bufalin, an active ingredient of ChanSu, induces adhesion of human leukemia cells, which may be related to lipid raft positioning [15]. However, whether CB regulates the development of lung cancer cells through lipid rafts is not clear.

Given the above findings, we assume that CB promotes the apoptosis of NSCLC cells by regulating lipid rafts to target lipid raft-related signal transduction.

## Material and methods

### Cell culture and treatment

Human bronchial epithelioid cell line 16HBE (CL-0249, Procell, China), along with NSCLC cell lines A549 (CL0016, Procell, China) and H1299 (CL0165, Procell, China), was separately cultured in Roswell Park Memorial Institute (RPMI)-1640 medium (72400120, GIBCO, USA) containing 10% fetal bovine serum (10091, Thermo Fisher, USA) and 1% penicillin streptomycin (15140-122, Thermo Fisher, USA) at 37°C with 5% CO<sub>2</sub> (Forma Steri-Cycle, Thermo Scientific, USA).

To probe the effect of CB (PHL89609, Merck, Germany) on NSCLC cells, NSCLC cells were treated by gradient concentrations of CB (0, 0.5, 1 and 2 μM) for 24 h [16].

### Transfection

A caveolin-1 overexpression vector was constructed by cloning the full-length sequence of caveolin-1 into pcDNA3.1+ vector (V87020, Thermo Fisher, USA). The transfection was completed with the help of Lipofectamine RNAiMAX (13778100, Thermo Fisher, USA) [17]. Twenty-four hours later, quantitative reverse transcription polymerase chain reaction (qRT-PCR) was carried out, by which the success of cell transfection was determined. To ascertain whether CB affected NSCLC cells by regulating caveolin-1, A549 or H1299 cells were transfected with negative control or caveolin-1 overexpression vector, and then treated with 2 μM CB for 24 h.

### 3-(4, 5-dimethylthiazol-2-yl)-2,5-diphenyl tetrazolium bromide (MTT) assay

An MTT kit (40206ES76, YEASEN, China) was used for detection of cell viability [18]. Briefly, A549 and H1299 cells were inoculated in the 96-well plates at a density of 5,000 cells/well and then cultivated with MTT working solution at 37°C for 4 h. Thereafter, the dissolving solution was added to further incubate the cells for 4 h. Finally, the absorbance at 570 nm was measured by a microplate reader (HBS-1096A, Sfmtit, China).

### Apoptosis

An Annexin V-Fluorescein Isothiocyanate (FITC)/Propidium Iodide (PI) apoptosis detection kit (40302ES20, YEASEN, China) was applied to examine cell apoptosis as previously reported [19]. Briefly, A549 and H1299 cells ( $5 \times 10^5$ ) were resuspended in binding buffer, and then reacted with 5 μl of Annexin V-FITC and 10 μl of PI at room temperature for 15 min. Afterwards, 400 μl of binding buffer was supplemented for dilution. Later, the cell suspension was collected and then put into a flow cytometer (DxFLEX, Beckman, USA) for detection of cell apoptosis.

### Western blot

Western blot was performed as previously described [20]. Specifically, the cells were lysed with Radio Immunoprecipitation Assay (RIPA) Lysis Buffer (20101ES60, YEASEN, China) and quantified by a Bicinchoninic acid (BCA) Protein Assay Kit (20201ES76, YEASEN, China). Then, the protein was separated and transferred to polyvinylidene fluoride (PVDF) membrane (YA1701, Solarbio, China). Subsequently, the membrane was treated by blocking solution (36100ES25, YEASEN, China) for 1 h. After washing, the membrane was sequentially incubated with primary antibodies and secondary antibodies. The primary antibodies adopted in this research included those against Bcl-2 (1 : 2000, 26 kDa, ab182858), Bax (1 : 1000, 21 kDa, ab32503), cleaved caspase-3 (1 : 500, 17 kDa, ab49822), cleaved caspase-9 (1 : 200, 37 kDa, ab2324), caveolin-1 (1 : 1000, 20 kDa, ab2910), FLOT 2 (1 : 1000, 47 kDa, ab96507), Akt (1 : 500, 56 kDa, ab8805), phosphor-Akt (p-Akt, ser473, 1 : 5000, 56 kDa, ab81283), p-Akt (thr308, 1 : 1000, 56 kDa, ab38449), and β-actin (1 : 1000, 42 kDa, ab8226). The secondary antibodies were horseradish peroxidase (HRP)-conjugated goat anti-rabbit IgG (1 : 5000, ab6721) and goat anti-mouse IgG (1 : 5000, ab6788). All these antibodies were purchased from Abcam (UK). β-actin was used as an internal control. The protein bands were visualized by iBright CL750 (Thermo Fisher, USA) with the assistance of Super ECL Detection Reagent (36208ES60, YEASEN, China).

### Detection of reactive oxygen species (ROS) level

The detection of ROS was carried out with a ROS detection kit (50101ES01, YEASEN, China) [21]. Cells ( $1 \times 10^6$ /ml) were reacted with the diluted 2,7-dichlorodi-hydrofluorescein diacetate (DCFH-DA), followed by being washed with serum-free 1640 medium. The results were recorded by the flow cytometer.

### Distribution of sphingomyelin and cholesterol in cells

BODIPY-labeled cholesterol analog (C12680, Thermo Fisher, USA) and sphingomyelin (D3522, Thermo Fisher, USA) were used to trace cholesterol and sphingomyelin. The operation was based on the research of Mishra *et al.* [22]. Simply put, the processed cells were resuspended in serum-free medium supplemented with the labeled cholesterol analog and sphingomyelin at 4°C for 0.5 h. After washing, cells were photographed using a microscope (400× magnification, FV3000, Olympus, Japan).

### Immunofluorescence

The immunofluorescence staining was conducted as previously documented [23]. A sterile glass slide was placed in 6-well plates and NSCLC cells were inoculated on the glass slide. After being immersed in fixing solution (E672002, Sangon, China) for 20 min, cells were permeabilized by Triton-X-100 (A110694, Sangon, China) for 15 min and blocked by blocking solution for 30 min. Subsequently, cells were reacted with anti-caveolin-1 antibody (1 : 50, ab185043, Abcam, UK) at 4°C overnight and counterstained with Hoechst staining solution (E607301, Sangon, China). Finally, a fluorescence microscope (IX73, Olympus, Japan) was employed to observe the distribution of caveolin-1 in cells.

### Lipid raft and non-lipid raft fractionation for protein analysis

Lipid rafts were isolated as previously instructed [24]. Briefly, cells were collected and lysed on ice. After centrifugation at 12,000 rpm/min for 10 min at 4°C, the cell supernatant was collected and mixed with 1 ml of 80% sucrose solution, followed by sequential addition of 30% sucrose (2.25 ml) and 5% sucrose (1.5 μl). Subsequently, the sucrose gradients were centrifuged ( $2 \times 10^5 \times g$ ) at 4°C for 18 h. Finally, 12 fractions (fractions 3–5 contained lipid rafts; fractions 10–12 were non-raft fractions) of proteins were collected and analyzed by Western blot.

### Quantitative reverse transcription polymerase chain reaction (qRT-PCR)

The total RNA was extracted by the RNA extraction kit (19231ES08, YEASEN, China). Reverse transcription and qPCR were completed in the same reaction tube under the help of a one-step RT-qPCR SYBR Green kit (11143ES50, YEASEN, China). The data were exhibited in the PCR Detection System (TP700, TaKaRa, Japan). The primers were as follows: caveolin-1 (forward: 5'-GCACAAGCTTTGCATGTCCA-3'; reverse: 5'-AGTACTCTGGGTAGGAGCAGA-3'); β-actin (forward: 5'-GGGACCTGACTGACTACCTC-3'; reverse: 5'-ACGCTTCACGAATTTGCGT-3'). β-actin acted as the reference gene. The relative gene expression was calculated using the  $2^{-\Delta\Delta Ct}$  method [25].

### Statistical analysis

Data were analyzed by Graph Prism v8.0 (GraphPad software, California, USA) and presented as mean ± standard deviation. One-way analysis of variance was used for comparison among multiple groups. Dunnett's post-hoc test results are shown in Figures 1 to 3, while Bonferroni's post-hoc test results are shown in the rest of the figures.  $P < 0.05$  was accepted as statistically significant.

## Results

### Effects of CB on NSCLC cell viability, apoptosis and ROS level

The chemical structure of CB is displayed in Figure 1 A. CB at gradient concentrations (0.5, 1 and 2 μM) was confirmed to attenuate the viability of NSCLC cells (Figures 1 B, C,  $p < 0.05$ ), and this inhibitory effect was more evident as the concentration of CB increased. However, CB had no significant effects on the viability of 16HBE cells (Figure 1 D). Furthermore, it was also proved that CB dose-dependently promoted NSCLC cell apoptosis (Figures 1 E, F,  $p < 0.001$ ) but barely affected the apoptosis of 16HBE cells (Figure 1 G). Then, the expression of apoptosis-related proteins was tested. The results revealed that as the concentration of CB increased, the protein expression of Bcl-2 was reduced, while that of Bax, cleaved caspase-3 and cleaved caspase-9 was augmented in NSCLC cells (Figure 1 H, I,  $p < 0.05$ ). As depicted in Figures 2 A, B, CB also dose-dependently increased the level of ROS in NSCLC cells.

### CB redistributed the lipid content on the membrane surface by regulating the expression of lipid raft-related proteins

Lipid rafts have been reported to occupy a pivotal position in the survival and death of cells [26].

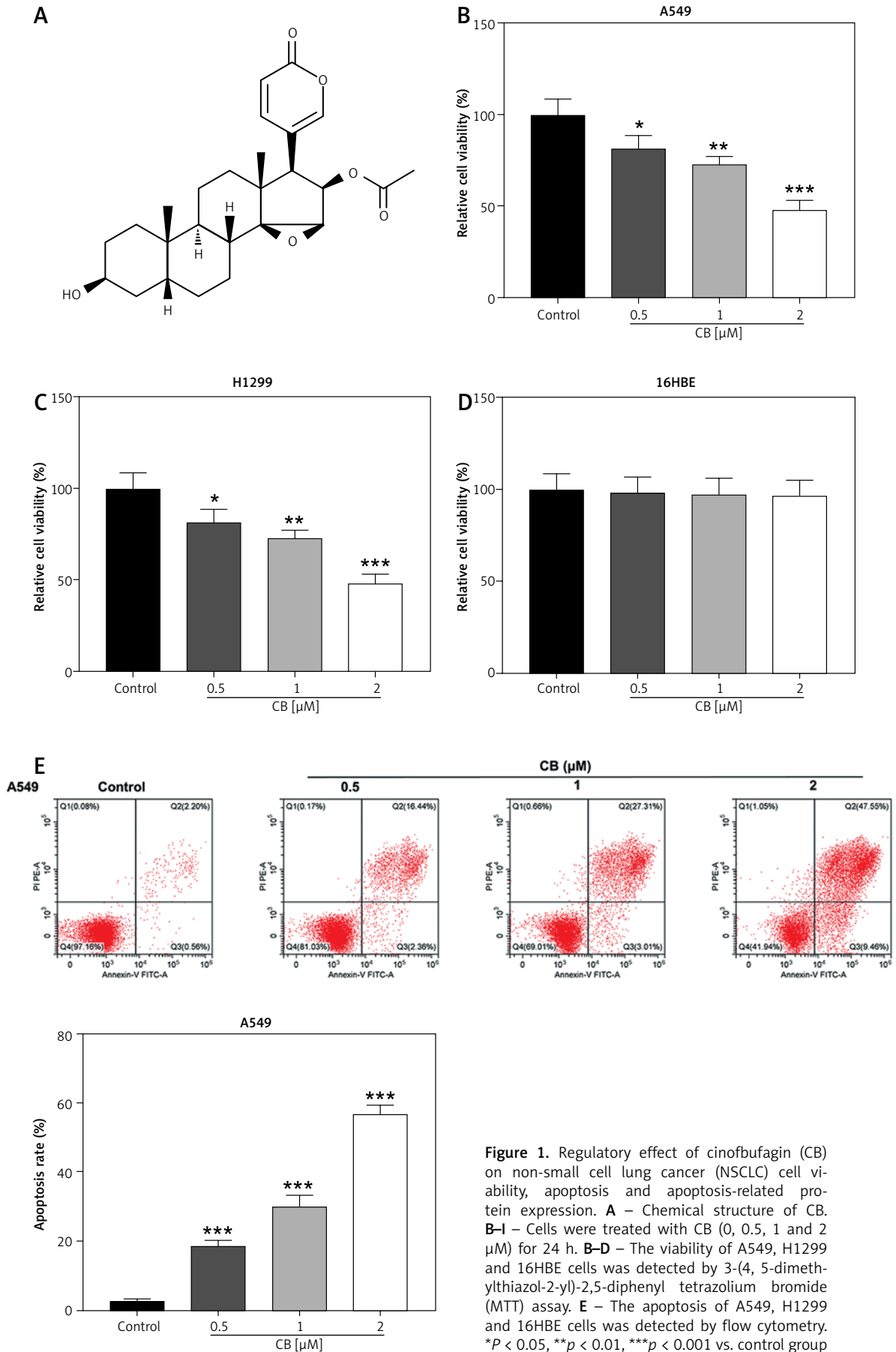


**Figure 1.** Regulatory effect of cinobufagin (CB) on non-small cell lung cancer (NSCLC) cell viability, apoptosis and apoptosis-related protein expression. **A** – Chemical structure of CB. **B–I** – Cells were treated with CB (0, 0.5, 1 and 2 μM) for 24 h. **B–D** – The viability of A549, H1299 and 16HBE cells was detected by 3-(4, 5-dimethylthiazol-2-yl)-2,5-diphenyl tetrazolium bromide (MTT) assay. **E** – The apoptosis of A549, H1299 and 16HBE cells was detected by flow cytometry. \* $P < 0.05$ , \*\* $p < 0.01$ , \*\*\* $p < 0.001$  vs. control group

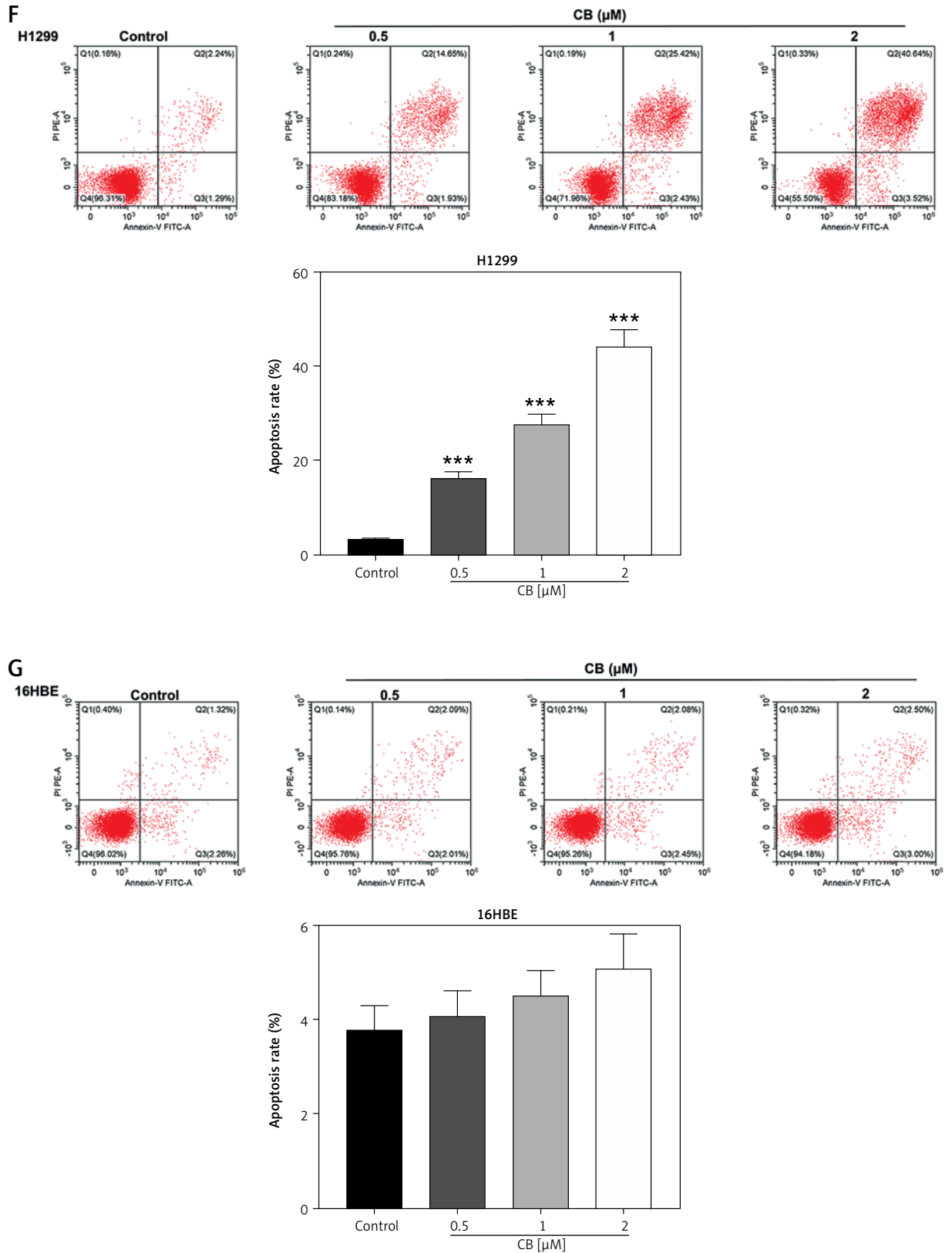


**Figure 1.** Cont. **F, G** – The apoptosis of A549, H1299 and 16HBE cells was detected by flow cytometry.. \* $P < 0.05$ , \*\* $p < 0.01$ , \*\*\* $p < 0.001$  vs. control group

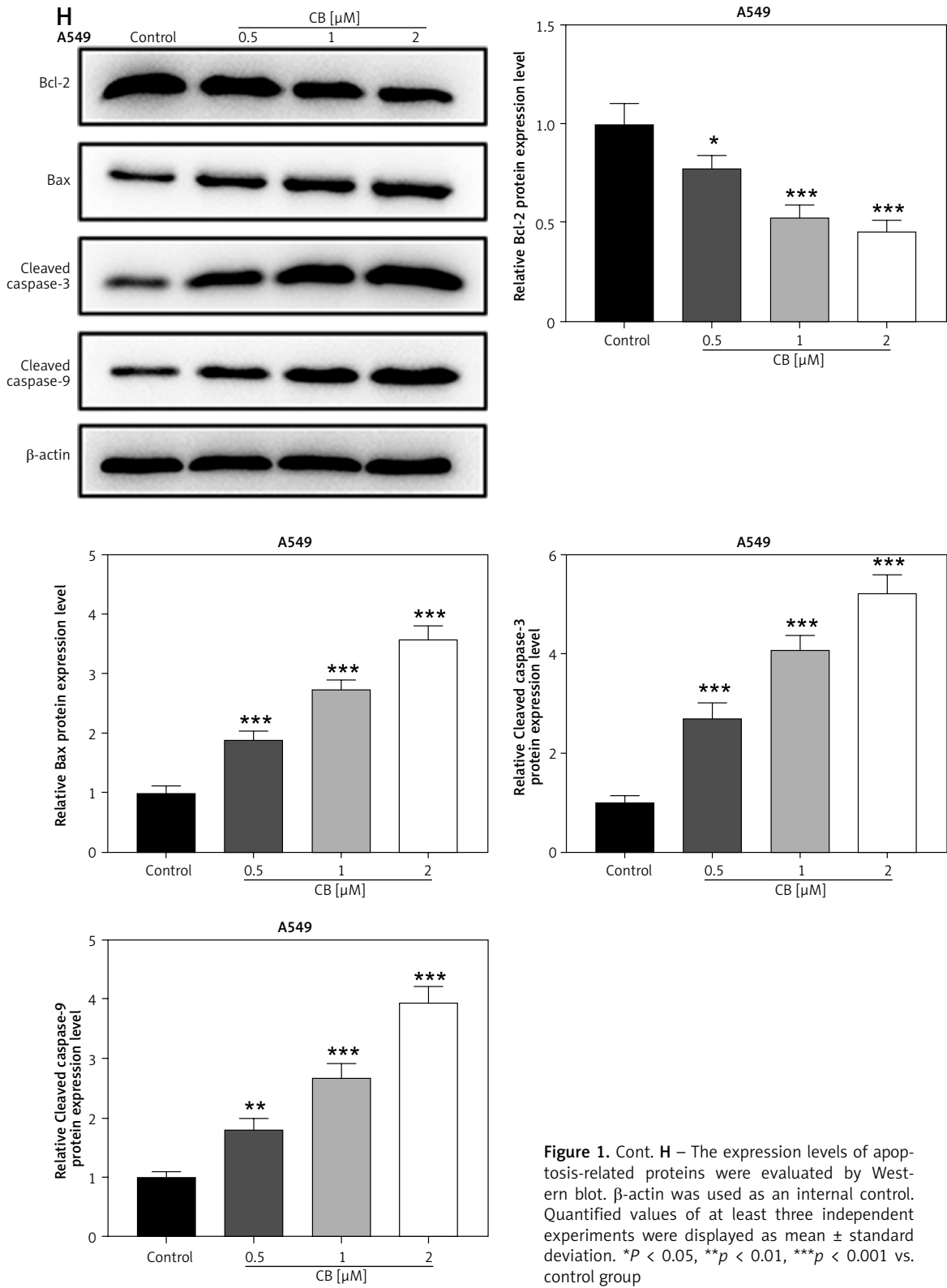


**Figure 1.** Cont. **H** – The expression levels of apoptosis-related proteins were evaluated by Western blot.  $\beta$ -actin was used as an internal control. Quantified values of at least three independent experiments were displayed as mean  $\pm$  standard deviation. \* $P < 0.05$ , \*\* $p < 0.01$ , \*\*\* $p < 0.001$  vs. control group

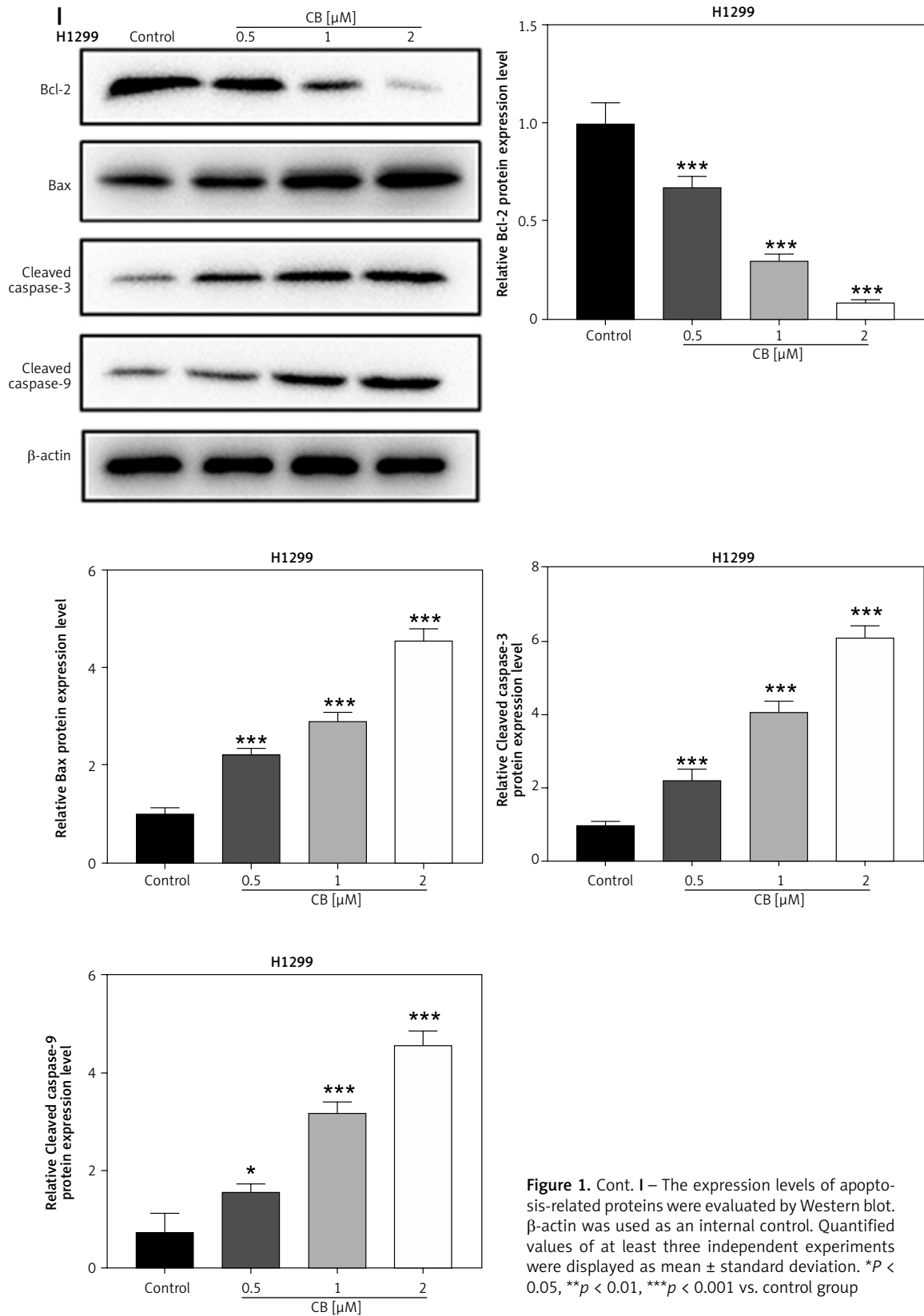


**Figure 1.** Cont. I – The expression levels of apoptosis-related proteins were evaluated by Western blot.  $\beta$ -actin was used as an internal control. Quantified values of at least three independent experiments were displayed as mean  $\pm$  standard deviation. \* $P < 0.05$ , \*\* $p < 0.01$ , \*\*\* $p < 0.001$  vs. control group

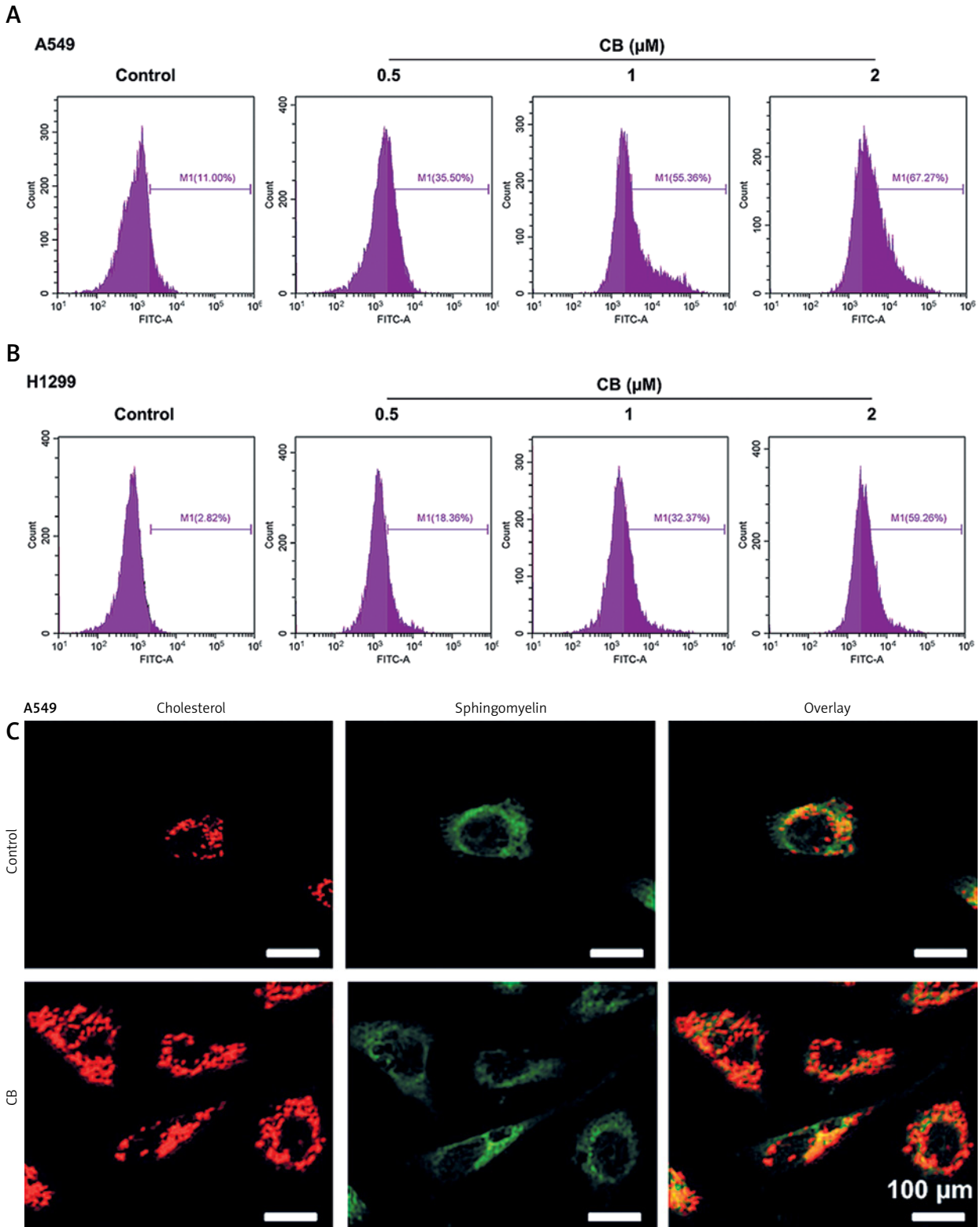


**Figure 2.** CB promoted the level of reactive oxygen species (ROS) and changed the distribution of cholesterol and sphingomyelin on the membrane surface. **A, B** – The level of ROS in A549 and H1299 cells treated with CB (0, 0.5, 1 and 2  $\mu\text{M}$ ) was measured by flow cytometry. **C** – The distribution of sphingomyelin and cholesterol was observed by a confocal microscope. Scale bar = 400  $\mu\text{m}$ . Quantified values of at least three independent experiments were expressed as mean  $\pm$  standard deviation

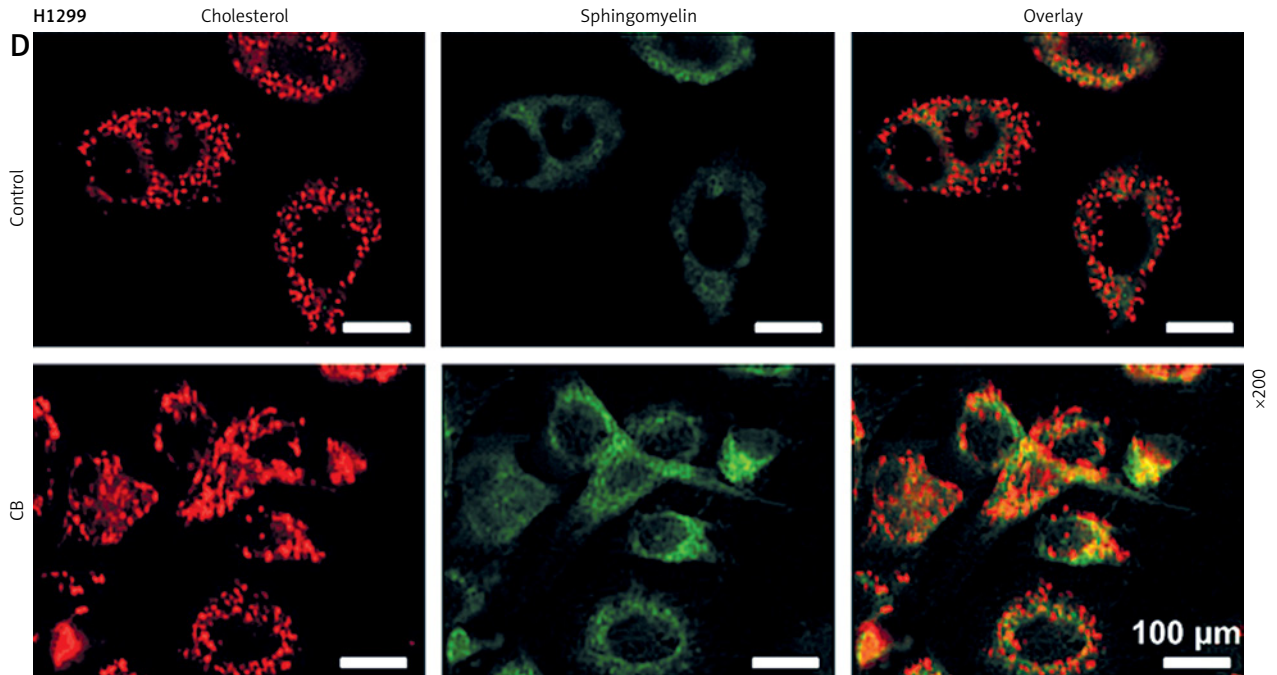


**Figure 2. Cont. D** – The distribution of sphingomyelin and cholesterol was observed by a confocal microscope. Scale bar = 400  $\mu$ m

In order to evaluate whether CB affects the biological behavior of NSCLC cells by regulating the lipid rafts, the changes in the distribution of cholesterol and sphingomyelin in cells were scrutinized before and after CB treatment. From Figures 2 C, D, it can be summarized that cholesterol and sphingomyelin were redistributed on the membrane surface after CB treatment. Also, the impacts of CB upon the expression of lipid raft-related proteins were evaluated. It was found that CB dose-dependently suppressed the expression of caveolin-1 and FLOT2, indicating that CB may destroy the integrity of the lipid rafts (Figures 3 A, B,  $p < 0.05$ ). The activation of Akt in lipid rafts was associated with the integrity of the lipid rafts [27], whilst CB was demonstrated to inhibit the level of p-Akt (Ser473 and Thr308) ( $p < 0.05$ ). Since 2  $\mu$ M CB exerted the most prominent effect, CB at this concentration was singled out for subsequent experiments. Immunofluorescence experiment results revealed that CB can restrain the expression of caveolin-1 in the cell membrane (Figures 3 C, D). Moreover, we isolated the lipid rafts (fractions 3–5) and non-raft fractions (fractions 10–12), and found that CB overtly inhibited the expression of caveolin-1 in lipid rafts and slightly restrained the expression of caveolin-1 in non-raft fractions (Figures 3 E, F).

**CB regulated NSCLC cell viability, apoptosis, ROS level, lipid content distribution, lipid raft-related protein expression and activation of Akt by inhibiting caveolin-1 expression**

To evaluate whether caveolin-1 participates in the effect of CB, caveolin-1 was overexpressed in

NSCLC cells. The results of both Western blot and qRT-PCR indicated that caveolin-1 overexpression reversed the inhibitory effects of CB on mRNA and protein levels of caveolin-1 (Figures 4 A–D,  $p < 0.05$ ), and also negated the effects of CB on suppressing cell viability (Figures 4 E, F,  $p < 0.001$ ) and promoting apoptosis (Figures 5 A, B,  $p < 0.001$ ). At the same time, overexpression of caveolin-1 offset the modulation of CB on apoptosis-related proteins Bcl-2, Bax, cleaved caspase-3 and cleaved caspase-9 (Figures 5 C, D,  $p < 0.05$ ). Moreover, the regulatory effects of CB on ROS level (Figures 6 A, B), lipid content distribution (Figures 6 C, D), lipid raft-related proteins (Figures 6 E, F,  $p < 0.001$ ), and phosphorylation of Akt (Figures 6 E, F,  $p < 0.05$ ) were all counteracted by caveolin-1 overexpression.

**Discussion**

CB has been proved to induce the apoptosis of NSCLC cells by regulating the AKT pathway [16]. Moreover, the effect of CB on the apoptosis of NSCLC cells is time-dependent, and apoptotic cells with broken nuclei can be observed after 24 h of CB treatment [16]. On this basis, in our study, the mechanism of CB affecting NSCLC cell apoptosis was revealed to be related to the down-regulation of caveolin-1, which destroys the lipid raft stability. Specifically, CB down-regulates caveolin-1 level to redistribute sphingomyelin and cholesterol in lipid rafts, leading to down-regulation of AKT pathway- and apoptosis-related markers in NSCLC cells. At the same time, our study also demonstrated that CB had no effect on the apoptosis and viability of 16HBE cells. To the best of our knowledge, this is the first study reporting the effect of CB on

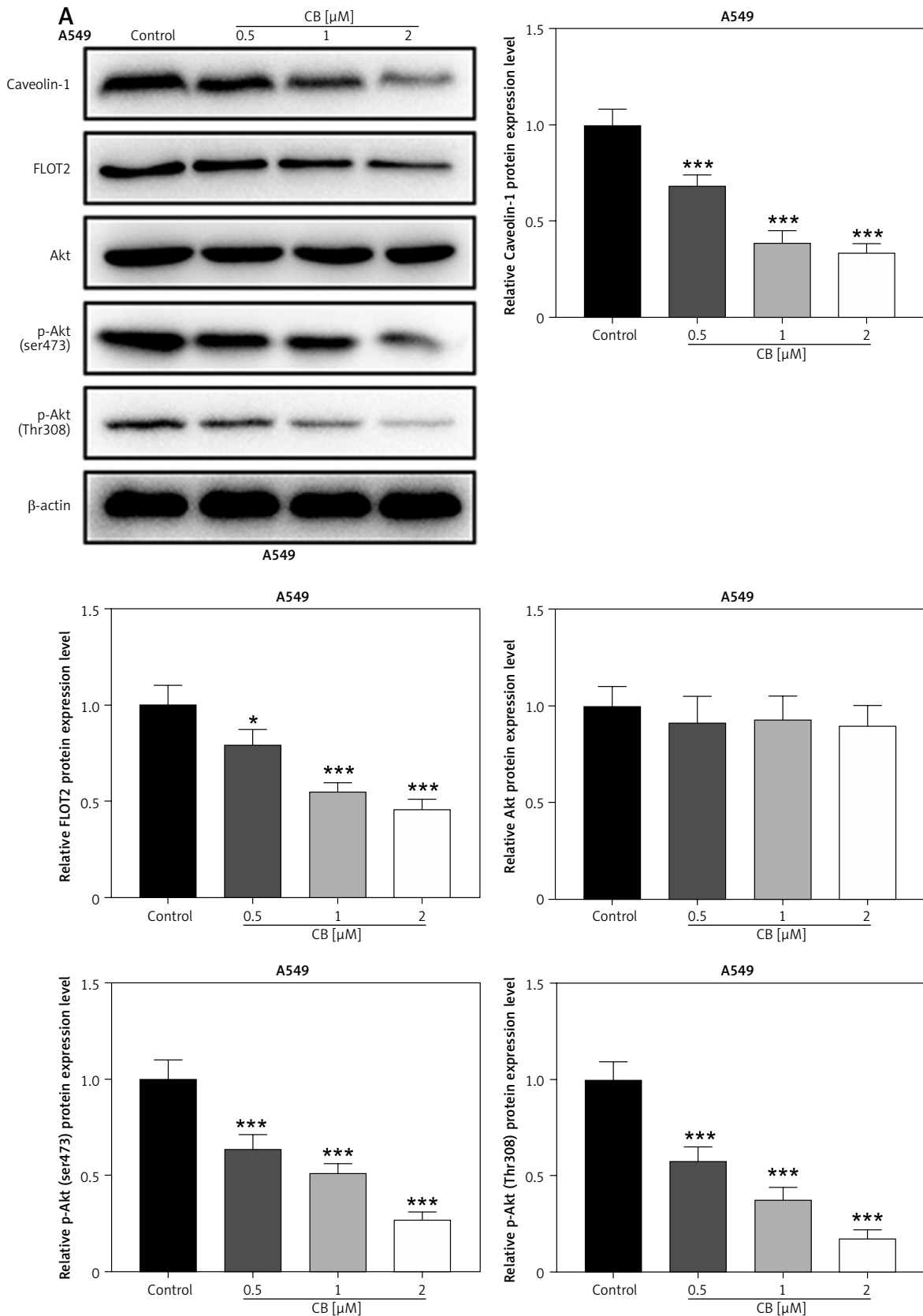


**Figure 3.** Effects of CB on expression of lipid raft-related proteins and phosphorylation of Akt. **A** – Expression levels of caveolin-1, flotillin 2 (FLOT2), Akt, and phosphor-Akt (p-Akt) in A549 and H1299 cells treated with CB (0, 0.5, 1 and 2  $\mu$ M) were measured by Western blot.  $\beta$ -actin was used as the internal control. Quantified values of at least three independent experiments were described as mean  $\pm$  standard deviation. \* $P$  < 0.05, \*\* $p$  < 0.01, \*\*\* $p$  < 0.001 vs. control group

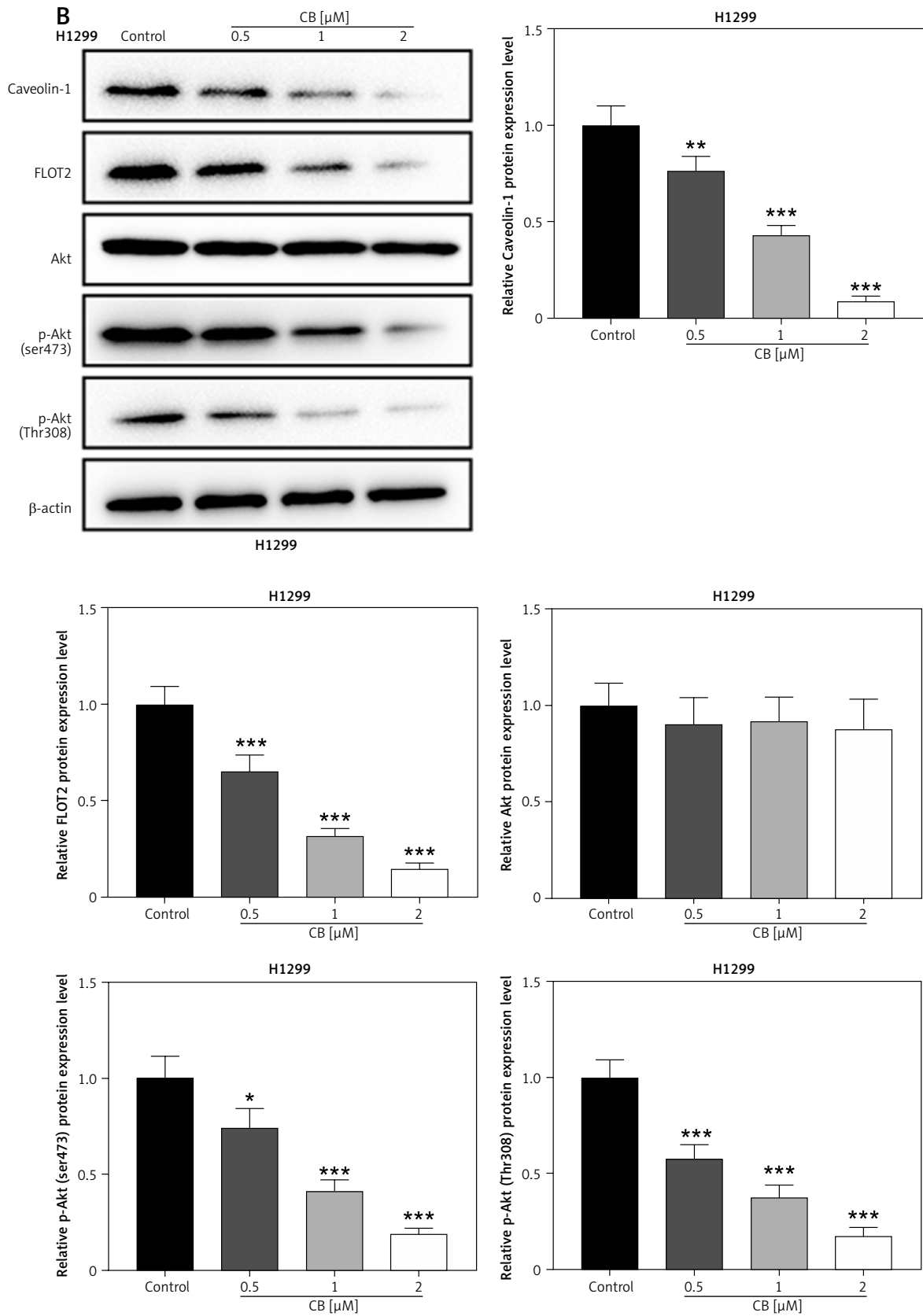


**Figure 3.** Cont. **B** – Expression levels of caveolin-1, flotillin 2 (FLOT2), Akt, and phosphor-Akt (p-Akt) in A549 and H1299 cells treated with CB (0, 0.5, 1 and 2  $\mu$ M) were measured by Western blot.  $\beta$ -actin was used as the internal control. \* $P < 0.05$ , \*\* $p < 0.01$ , \*\*\* $p < 0.001$  vs. control group

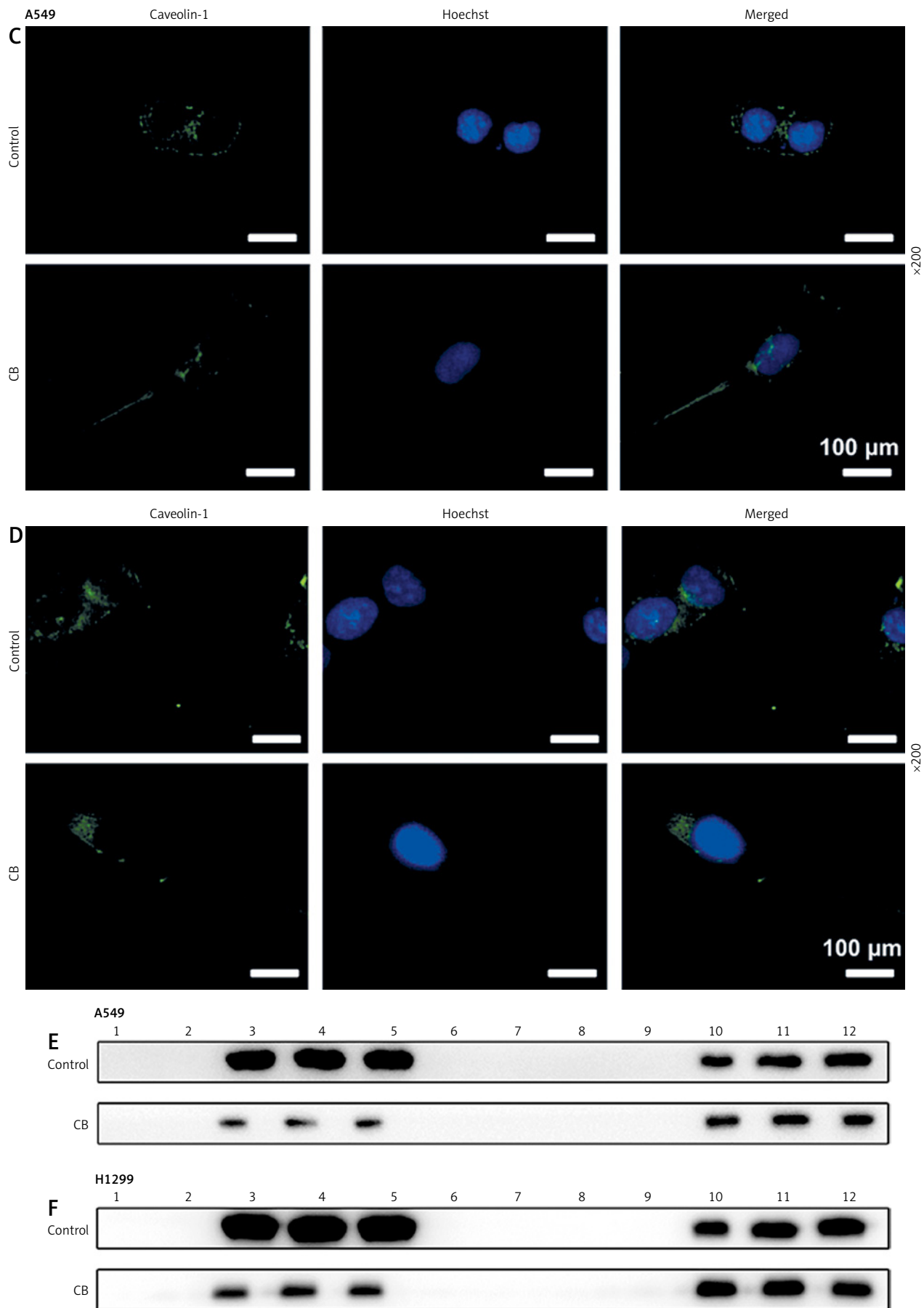


**Figure 3.** Cont. **C, D** – Immunofluorescence detection of 2  $\mu\text{M}$  CB on the distribution of lipid raft marker caveolin-1 in cells. Scale bar = 400  $\mu\text{m}$ . **E, F** – The distribution of caveolin-1 in lipid rafts (3–5) and non-raft fractions (10–12) of A549 and H1299 cells treated with 2  $\mu\text{M}$  CB. Quantified values of at least three independent experiments were described as mean  $\pm$  standard deviation. \* $P < 0.05$ , \*\* $p < 0.01$ , \*\*\* $p < 0.001$  vs. control group

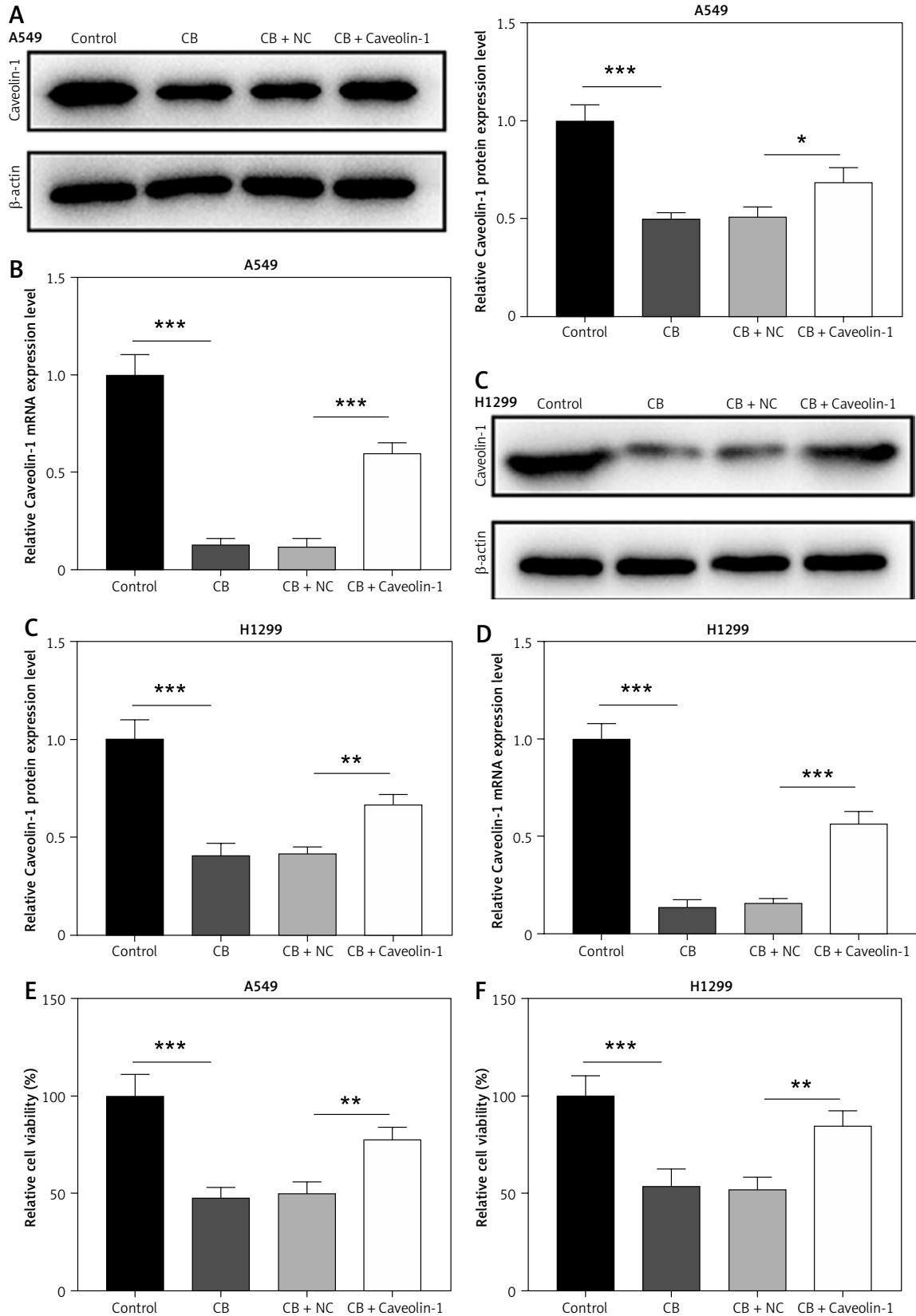


**Figure 4.** Overexpression of caveolin-1 reversed the inhibitory effects of CB on caveolin-1 protein level and viability of NSCLC cells. A549 or H1299 cells were transfected with negative control (NC) or caveolin-1 overexpression vector, followed by treatment of 2  $\mu$ M CB for 24 h. **A–D** – Western blot and quantitative reverse transcription polymerase chain reaction (qRT-PCR) were applied to detect caveolin-1 mRNA and protein expression in cells of each group.  $\beta$ -actin was used as the internal control. **E, F** – MTT assay was conducted to determine the viability of cells in each group. Quantified values of at least three independent experiments were presented as mean  $\pm$  standard deviation. \* $P$  < 0.05, \*\* $p$  < 0.01, \*\*\* $p$  < 0.001 vs. control group or CB + NC group

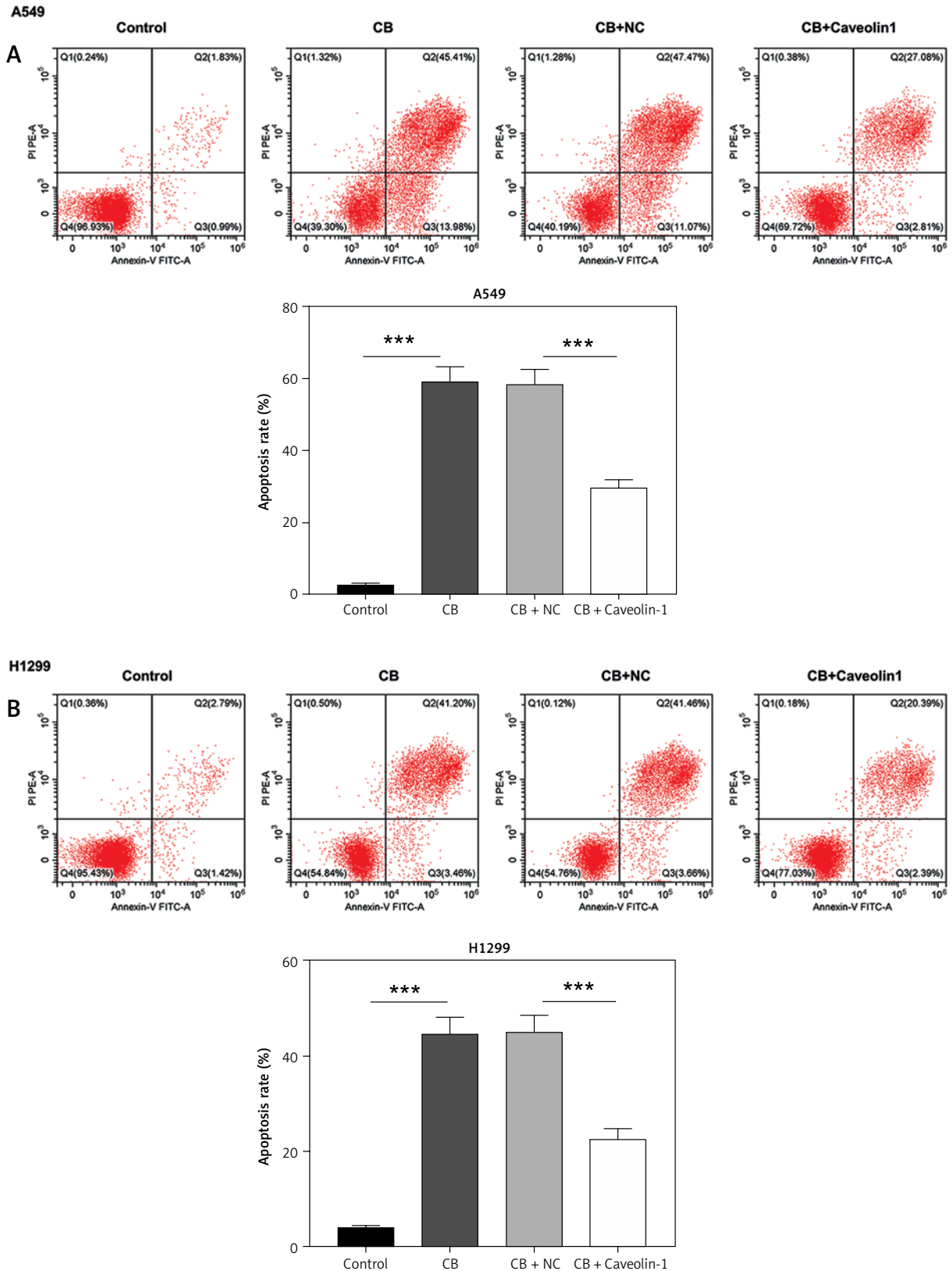


**Figure 5.** Caveolin-1 overexpression reversed the effects of CB on NSCLC cell apoptosis and the expression of apoptosis-related proteins. A549 or H1299 cells were transfected with NC or caveolin-1 overexpression vector and then treated with 2  $\mu$ M CB for 24 h. **A, B** – The apoptosis of cells in each group was detected by flow cytometry. \* $P < 0.05$ , \*\* $p < 0.01$ , \*\*\* $p < 0.001$  vs. control group or CB + NC group

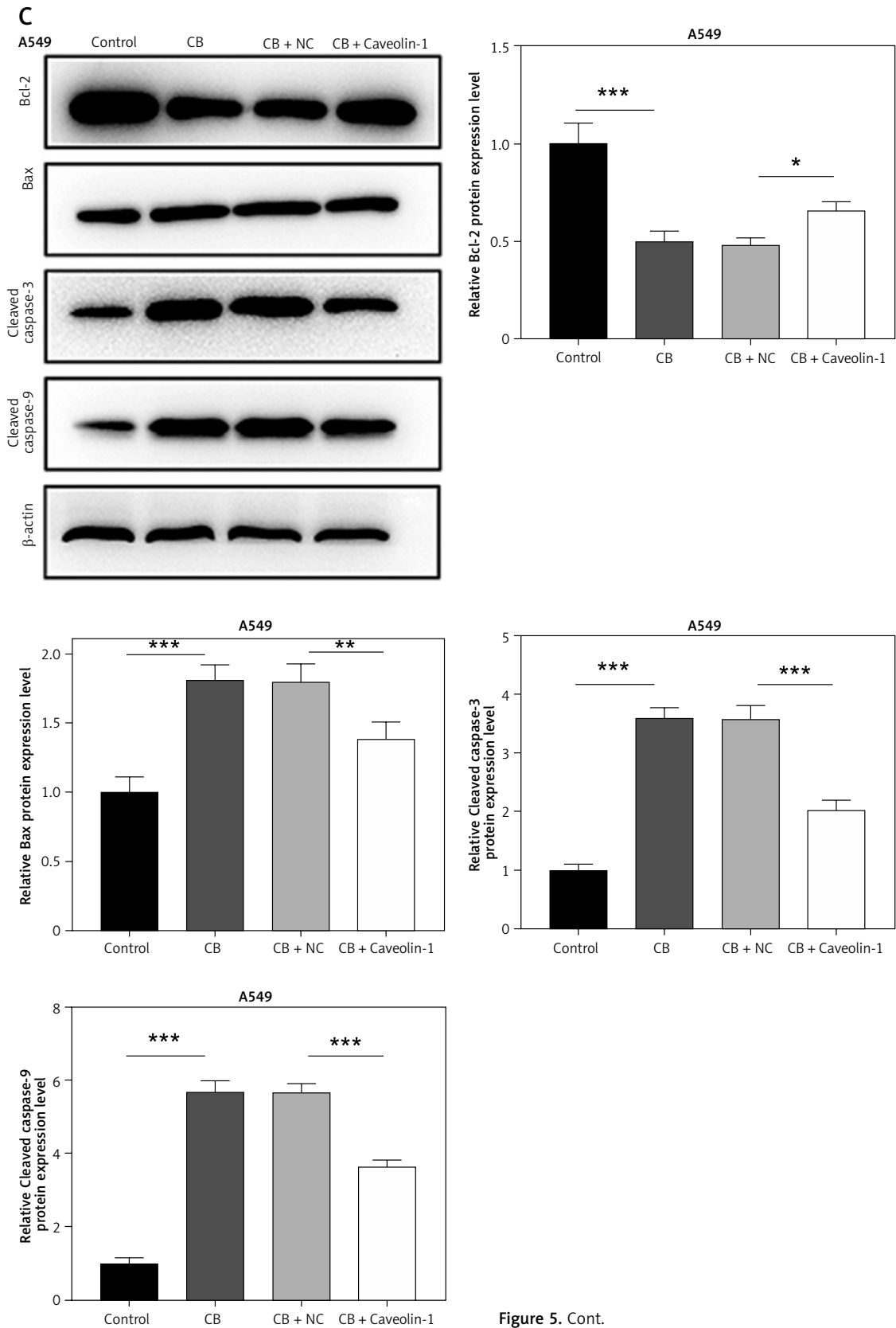
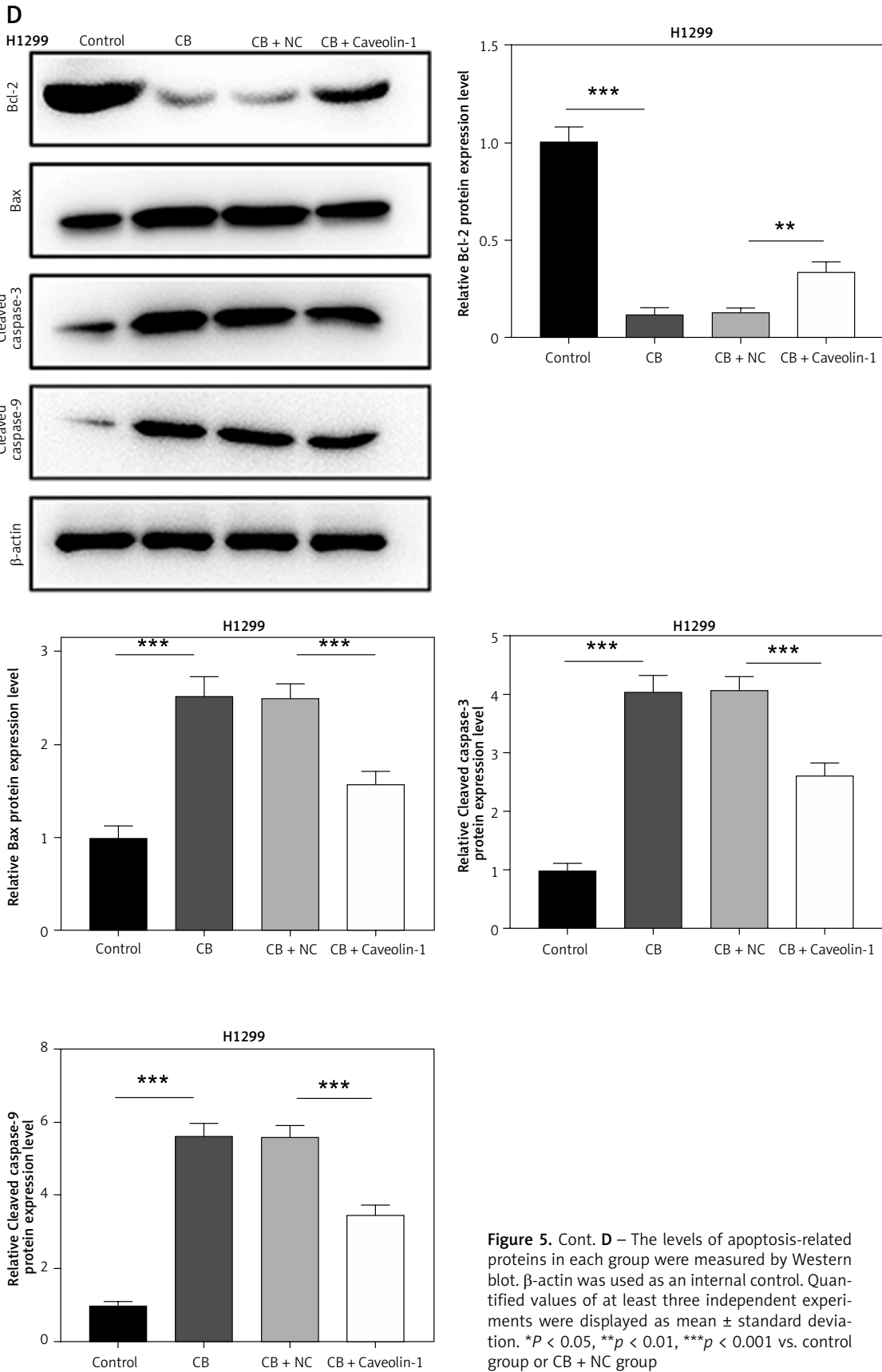
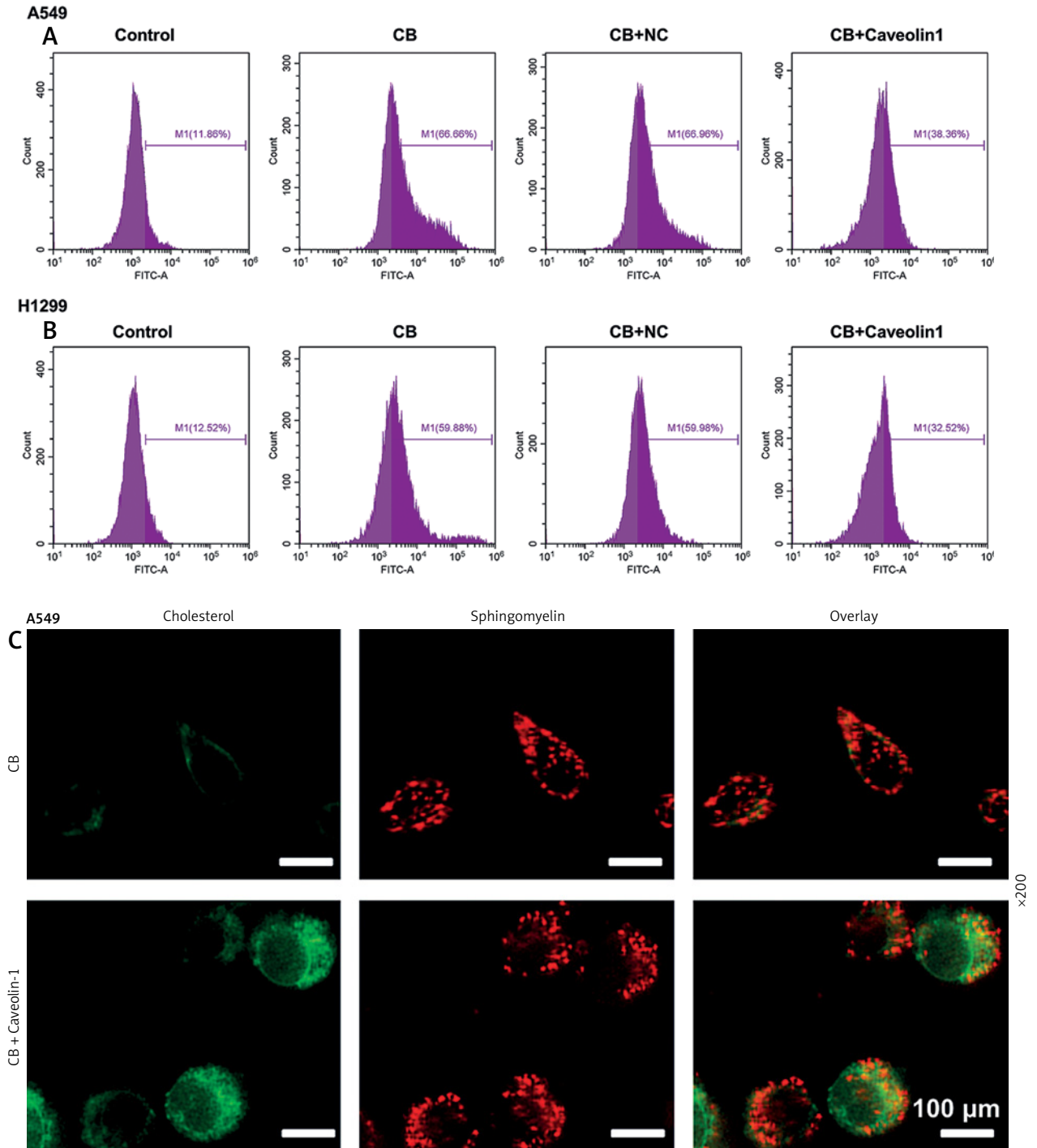


Figure 5. Cont.

**Figure 5. Cont. C** – The levels of apoptosis-related proteins in each group were measured by Western blot.  $\beta$ -actin was used as an internal control. Quantified values of at least three independent experiments were displayed as mean  $\pm$  standard deviation. \* $P$  < 0.05, \*\* $p$  < 0.01, \*\*\* $p$  < 0.001 vs. control group or CB + NC group



**Figure 5. Cont. D** – The levels of apoptosis-related proteins in each group were measured by Western blot.  $\beta$ -actin was used as an internal control. Quantified values of at least three independent experiments were displayed as mean  $\pm$  standard deviation. \* $P < 0.05$ , \*\* $p < 0.01$ , \*\*\* $p < 0.001$  vs. control group or CB + NC group



**Figure 6.** Caveolin-1 reversed the effects of CB on level of ROS, distribution of cholesterol and sphingomyelin as well as expression of FLOT2 and p-Akt. A549 or H1299 cells were subjected to transfection of NC or caveolin-1 over-expression vector, followed by treatment of 2  $\mu$ M CB for 24 h. **A, B** – The level of ROS in cells of each group was detected by flow cytometry. **C** – The images of the distribution of sphingomyelin and cholesterol in each group were captured by a confocal microscope (Scale bar = 400  $\mu$ m). \* $P < 0.05$ , \*\*\* $p < 0.001$  vs. control group or CB + NC group

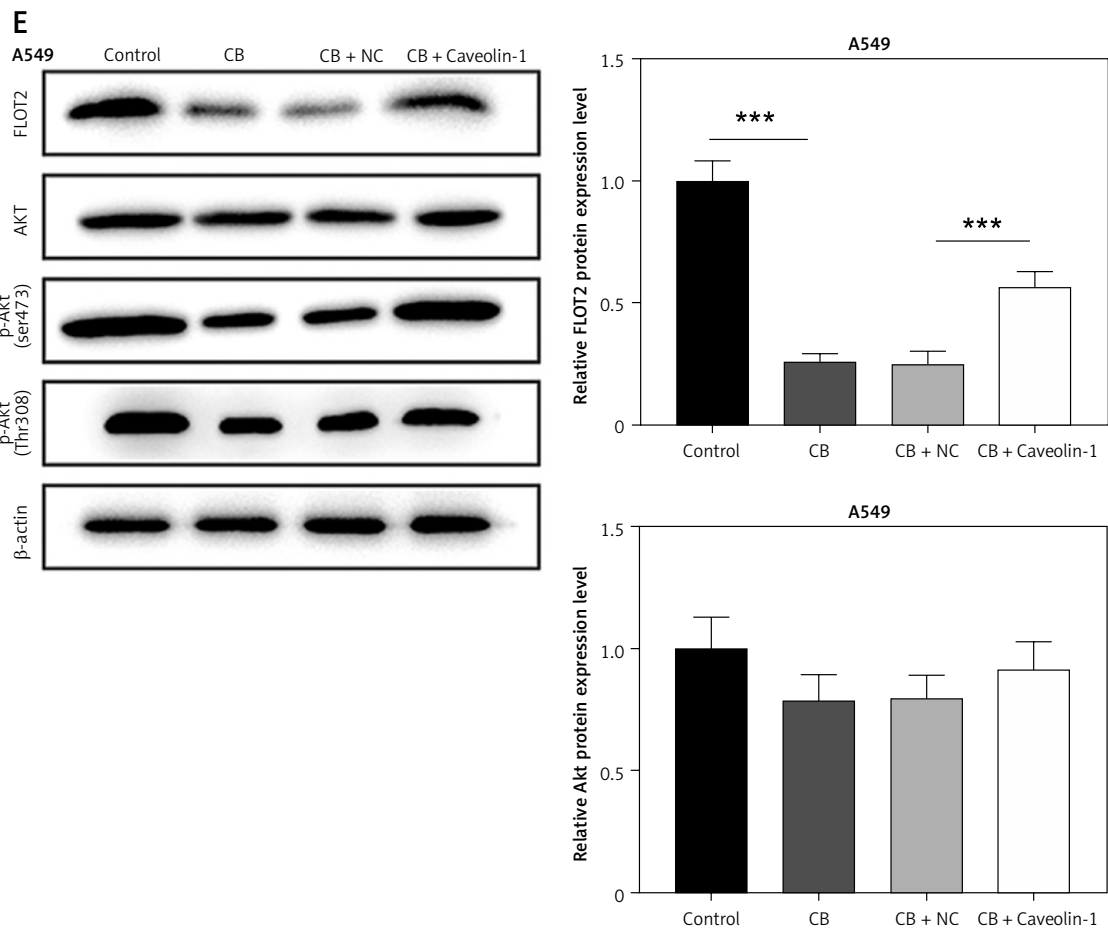
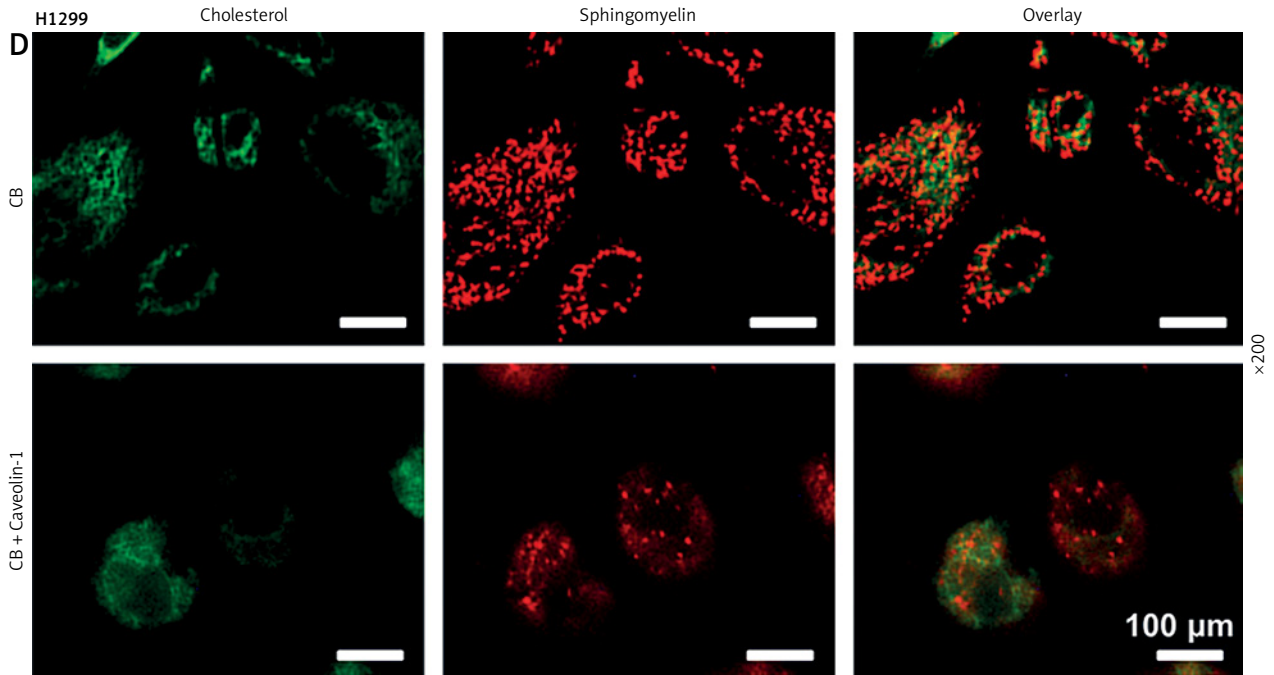


**Figure 6.** Cont. **D** – The images of the distribution of sphingomyelin and cholesterol in each group were captured by a confocal microscope (Scale bar = 400 μm). **E** – The levels of FLOT2, Akt, and p-Akt in A549 and H1299 cells were tested by Western blot. β-actin was used as the internal control. Quantified values of at least three independent experiments were described as mean ± standard deviation. \**P* < 0.05, \*\*\**p* < 0.001 vs. control group or CB + NC group

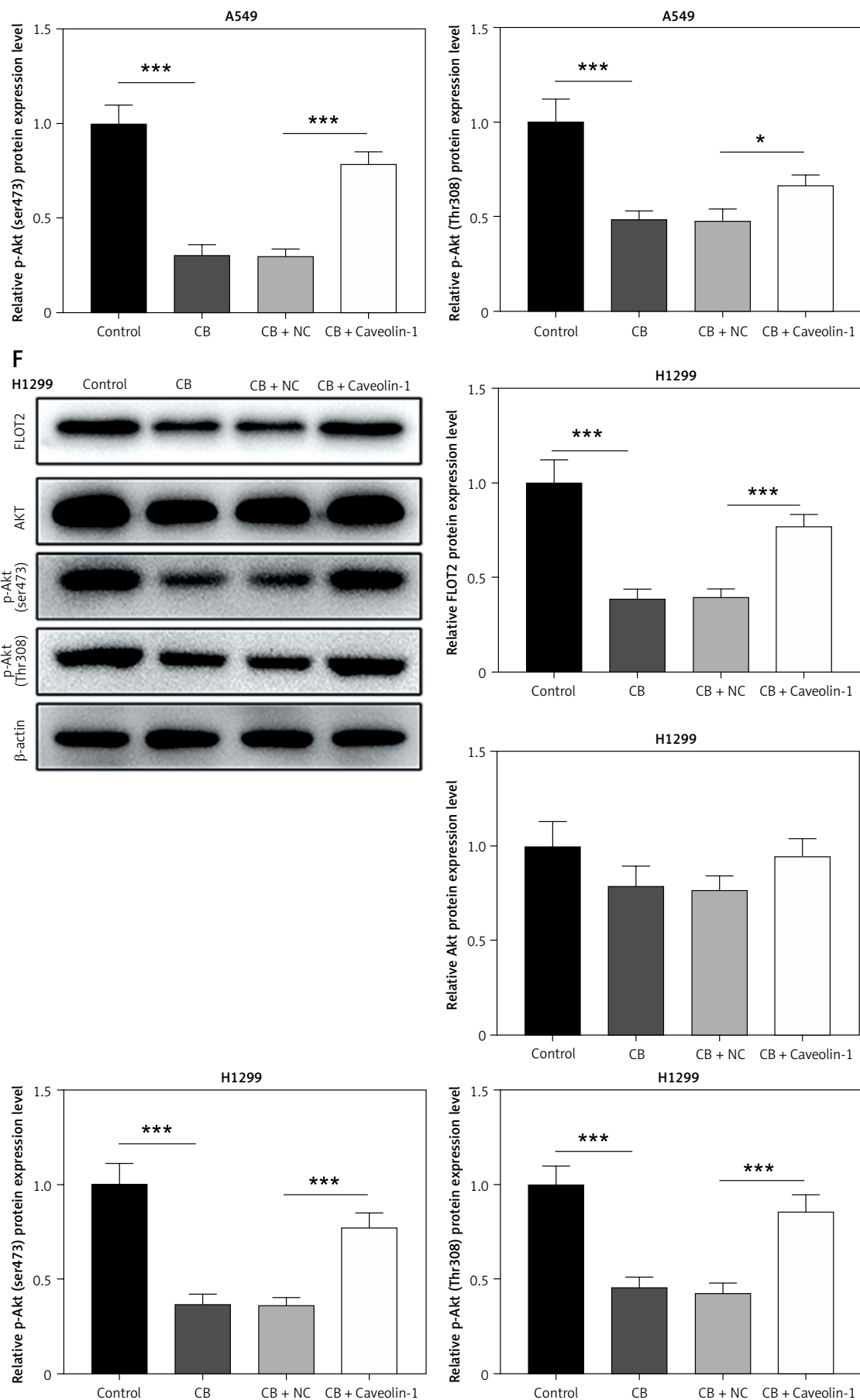


**Figure 6.** Cont. F – The levels of FLOT2, Akt, and p-Akt in A549 and H1299 cells were tested by Western blot. β-actin was used as the internal control. Quantified values of at least three independent experiments were described as mean ± standard deviation. \* $P < 0.05$ , \*\*\* $p < 0.001$  vs. control group or CB + NC group

undermining the integrity of lipid rafts by inducing the reduction of cholesterol in lipid rafts and the down-regulation of caveolin-1.

Studies have found that cancer cells contain more lipid rafts than normal cells, so regulating the lipid rafts to affect the death of cancer cells has potential therapeutic significance [27]. Lipid rafts are rich in sphingolipids and cholesterol, which can be damaged by changing the level of cholesterol or degrading the sphingolipids in the cell membrane. Mishra *et al.* suggested that cedrol impinges on the integrity of lipid rafts by modulating the redistributions of cholesterol and sphingomyelin, thus triggering the apoptosis of cancer cells [22]. In this study, we observed that CB can change the distribution of cholesterol and sphingomyelin in NSCLC cells, indicating that the anti-cancer function of CB may be related to the regulation of lipid rafts.

A more widely accepted hypothesis is that the components of lipid rafts, including cholesterol and sphingomyelin, will change as different proteins and cell molecules gather in the micro region. In this study, CB could partially change the level of caveolin-1 in lipid rafts, signifying that the regulatory effect of CB on the stability of lipid rafts was associated with the down-regulation of caveolin-1 in lipid rafts. Caveolin-1 is a vital marker of caveolae on lipid rafts. A decrease in the proportion of caveolin-1 will lead to the destruction of the integrity of the lipid raft, which is necessary for the survival of cancer cells [28]. Studies have confirmed that caveolin-1 is differentially expressed in various tumors [29]. Remarkably, high expression of caveolin-1 has a close relation with the aggressiveness and radiation resistance of lung cancer cells [30]. In addition, Wang *et al.* reported that RANKL-induced migration of gastric cancer cells is at least partially dependent on lipid rafts and their major component, caveolin-1, and is promoted by activation of c-Src and caveolin-1 [31]. The inhibition of caveolin-1 has been proved to enhance the apoptosis of NSCLC cells [32]. The inhibitory effect of caveolin-1 on cancer cell apoptosis seems to be related to the negative regulation of TRAIL [33], a gene that may induce specific apoptosis of cancer cells [34]. Similar to previous studies, we found that the overexpression of caveolin-1 reversed the promoting effect of CB on the apoptosis of NSCLC cells, implying that CB played an anti-cancer role by down-regulating the caveolin-1 level to disrupt the stability of the lipid raft.

In the cancer field, many survival-related pathways have been proven to be associated with lipid rafts, such as the AKT pathway [27]. AKT, a serine/threonine protein kinase, can mediate the survival signal of cells. When the activity of Akt was intensified, p-Akt at thr308 and ser473 sites was

activated to prevent NSCLC cells from undergoing apoptosis [35]. When the lipid raft domain is destroyed, the phosphorylation level of Akt will also be affected [36]. In this study, CB could hinder the activation of the AKT pathway in NSCLC cells, which is consistent with a previously reported conclusion that CB can impede AKT activation in melanoma cells [37], hepatocellular carcinoma cells [38] and NSCLC cells [16]. In addition, studies have also revealed that caveolin-1 can activate the AKT pathway, and blocking the caveolin-1/AKT pathway can enhance the apoptosis of NSCLC cells [32, 39]. The effect of caveolin-1 on AKT activation may be related to its interaction with and inhibition of serine/threonine protein phosphatase PP1 and PP2A through the binding site of the scaffold domain [40]. Interestingly, we found that caveolin-1 neutralized the regulation of p-AKT protein by CB, indicating that CB inhibited the expression of p-AKT protein by down-regulating the caveolin-1 level.

However, this study has some limitations. A prior study reported that FLOT is overexpressed in multiple cancers [41]. Also, Zhu *et al.* stated that Pulsatilla saponin E affects the activity of Akt by repressing the FLOT-2 level to promote the apoptosis of NSCLC cells [42]. Similarly, we have demonstrated that CB can down-regulate the expression of FLOT-2. Nevertheless, whether CB depends on FLOT2 to exert anti-cancer effects has not been confirmed yet. In addition, our research was confined to the mechanism of CB against NSCLC at the cellular level, and further verification is required in subsequent *in vivo* experiments. It is necessary to carry out similar experiments on other members of cardiac glycosides other than CB, so as to understand whether this is a specific effect brought on by CB.

In conclusion, collectively, our research proves that CB destroys the stability of lipid rafts by suppressing the expression of caveolin1 in lipid rafts, which leads to the inactivation of the AKT pathway, thus promoting cell apoptosis. In addition, CB can inhibit cancer cells without damaging normal cells, suggesting its great potential as an anti-cancer drug. Our findings may provide a new theoretical basis for the anti-cancer application of CB and bring a broad prospect for the treatment of NSCLC.

### Acknowledgments

Zhongqing Xu, Jinwei Li contributed equally to this work.

### Funding

This work was supported by the Subject of Shanghai Changning District Health Commission [20214Y003].

## Ethical approval

Not applicable.

## Conflict of interest

The authors declare no conflict of interest.

## References

- Hirsch FR, Scagliotti GV, Mulshine JL, et al. Lung cancer: current therapies and new targeted treatments. *Lancet* 2017; 389: 299-311.
- Evison M. The current treatment landscape in the UK for stage III NSCLC. *Br J Cancer* 2020; 123 (Suppl 1): 3-9.
- So TH, Chan SK, Lee VH, et al. Chinese medicine in cancer treatment – how is it practised in the East and the West? *Clin Oncol (R Coll Radiol)* 2019; 31: 578-88.
- Liu Y, Yang S, Wang K, et al. Cellular senescence and cancer: focusing on traditional Chinese medicine and natural products. *Cell Prolif* 2020; 53: e12894.
- Li X, Bi Z, Liu S, et al. Antifibrotic mechanism of cinobufagin in bleomycin-induced pulmonary fibrosis in mice. *Front Pharmacol* 2019; 10: 1021.
- Li F J, Hu J H, Ren X, et al. Toad venom: a comprehensive review of chemical constituents, anticancer activities, and mechanisms. *Arch Pharm (Weinheim)* 2021; 354: e2100060.
- Cao Y, Yu L, Dai G, et al. Cinobufagin induces apoptosis of osteosarcoma cells through inactivation of Notch signaling. *Eur J Pharmacol* 2017; 794: 77-84.
- Pan Z, Luo Y, Xia Y, et al. Cinobufagin induces cell cycle arrest at the S phase and promotes apoptosis in nasopharyngeal carcinoma cells. *Biomed Pharmacother* 2020; 122: 109763.
- Kim GH, Fang XQ, Lim WJ, et al. Cinobufagin suppresses melanoma cell growth by inhibiting LEF1. *Int J Mol Sci* 2020; 21: 6706.
- Li X, Chen C, Dai Y, et al. Cinobufagin suppresses colorectal cancer angiogenesis by disrupting the endothelial mammalian target of rapamycin/hypoxia-inducible factor 1 $\alpha$  axis. *Cancer Sci* 2019; 110: 1724-34.
- Xie M, Chen X, Qin S, et al. Clinical study on thalidomide combined with cinobufagin to treat lung cancer cachexia. *J Cancer Res Ther* 2018; 14: 226-32.
- Levental I, Levental KR, Heberle FA. Lipid rafts: controversies resolved, mysteries remain. *Trends Cell Biol* 2020; 30: 341-53.
- Sezgin E, Levental I, Mayor S, et al. The mystery of membrane organization: composition, regulation and roles of lipid rafts. *Nat Rev Mol Cell Biol* 2017; 18: 361-74.
- Jeon JH, Kim SK, Kim HJ, et al. Lipid raft modulation inhibits NSCLC cell migration through delocalization of the focal adhesion complex. *Lung Cancer* 2010; 69: 165-71.
- Qu X, Liu Y, Ma Y, et al. Up-regulation of the Cbl family of ubiquitin ligases is involved in ATRA and bufalin-induced cell adhesion but not cell differentiation. *Biochem Biophys Res Commun* 2008; 367: 183-9.
- Zhang G, Wang C, Sun M, et al. Cinobufagin inhibits tumor growth by inducing intrinsic apoptosis through AKT signaling pathway in human nonsmall cell lung cancer cells. *Oncotarget* 2016; 7: 28935-46.
- Dong C, Gongora R, Sosulski ML, et al. Regulation of transforming growth factor-beta1 (TGF- $\beta$ 1)-induced pro-fibrotic activities by circadian clock gene BMAL1. *Respir Res* 2016; 17: 4.
- Kumar P, Nagarajan A, Uchil PD. Analysis of cell viability by the MTT assay. *Cold Spring Harb Protoc* 2018; 2018(6).
- Kumar R, Saneja A, Panda AK. An annexin V-FITC-propidium iodide-based method for detecting apoptosis in a non-small cell lung cancer cell line. *Methods Mol Biol* 2021; 2279: 213-23.
- Pillai-Kastoori L, Schutz-Geschwender AR, Harford JA. A systematic approach to quantitative Western blot analysis. *Anal Biochem* 2020; 593: 113608.
- Ding J, Yao Y, Li J, et al. A reactive oxygen species scavenging and O(2) generating injectable hydrogel for myocardial infarction treatment in vivo. *Small* 2020; 16: e2005038.
- Mishra SK, Bae YS, Lee YM, et al. Sesquiterpene alcohol cedrol chemosensitizes human cancer cells and suppresses cell proliferation by destabilizing plasma membrane lipid rafts. *Front Cell Dev Biol* 2020; 8: 571676.
- Niu J, Wang J, Zhang Q, et al. Cinobufagin-induced DNA damage response activates G(2)/M checkpoint and apoptosis to cause selective cytotoxicity in cancer cells. *Cancer Cell Int* 2021; 21: 446.
- Ediriweera MK, Moon JY, Nguyen YT, et al. 10-gingerol targets lipid rafts associated PI3K/Akt signaling in radio-resistant triple negative breast cancer cells. *Molecules* 2020; 25: 3164.
- Livak KJ, Schmittgen TD. Analysis of relative gene expression data using real-time quantitative PCR and the 2(-Delta Delta C(T)) method. *Methods* 2001; 25: 402-8.
- Luo X, Cheng C, Tan Z, et al. Emerging roles of lipid metabolism in cancer metastasis. *Mol Cancer* 2017; 16: 76.
- Li B, Qin Y, Yu X, et al. Lipid raft involvement in signal transduction in cancer cell survival, cell death and metastasis. *Cell Prolif* 2022; 55: e13167.
- Badana A, Chintala M, Varikuti G, et al. Lipid raft integrity is required for survival of triple negative breast cancer cells. *J Breast Cancer* 2016; 19: 372-84.
- Ketteler J, Klein D. Caveolin-1, cancer and therapy resistance. *Int J Cancer* 2018; 143: 2092-104.
- Leiser D, Samanta S, Eley J, et al. Role of caveolin-1 as a biomarker for radiation resistance and tumor aggression in lung cancer. *PLoS One* 2021; 16: e0258951.
- Wang Y, Song Y, Che X, et al. Caveolin-1 enhances RANKL-induced gastric cancer cell migration. *Oncol Rep* 2018; 40: 1287-96.
- Philips BJ, Kumar A, Burki S, et al. Triptolide-induced apoptosis in non-small cell lung cancer via a novel miR204-5p/Caveolin-1/Akt-mediated pathway. *Oncotarget* 2020; 11: 2793-806.
- Zhao X, Liu Y, Ma Q, et al. Caveolin-1 negatively regulates TRAIL-induced apoptosis in human hepatocarcinoma cells. *Biochem Biophys Res Commun* 2009; 378: 21-6.
- Zinnah KMA, Park SY. Sensitizing TRAIL-resistant A549 lung cancer cells and enhancing TRAIL-induced apoptosis with the antidepressant amitriptyline. *Oncol Rep* 2021; 46: 144.
- Tan AC. Targeting the PI3K/Akt/mTOR pathway in non-small cell lung cancer (NSCLC). *Thorac Cancer* 2020; 11: 511-8.
- Calay D, Vind-Kezunovic D, Frankart A, et al. Inhibition of Akt signaling by exclusion from lipid rafts in normal and transformed epidermal keratinocytes. *J Invest Dermatol* 2010; 130: 1136-45.
- Pan Z, Zhang X, Yu P, et al. Cinobufagin induces cell cycle arrest at the G2/M phase and promotes apoptosis in malignant melanoma cells. *Front Oncol* 2019; 9: 853.

38. Yang AL, Wu Q, Hu ZD, et al. A network pharmacology approach to investigate the anticancer mechanism of cinobufagin against hepatocellular carcinoma via downregulation of EGFR-CDK2 signaling. *Toxicol Appl Pharmacol* 2021; 431: 115739.
39. Huang G, Lou T, Pan J, et al. MiR-204 reduces cisplatin resistance in non-small cell lung cancer through suppression of the caveolin-1/AKT/Bad pathway. *Aging (Albany NY)* 2019; 11: 2138-50.
40. Li L, Ren CH, Tahir SA, et al. Caveolin-1 maintains activated Akt in prostate cancer cells through scaffolding domain binding site interactions with and inhibition of serine/threonine protein phosphatases PP1 and PP2A. *Mol Cell Biol* 2003; 23: 9389-404.
41. Gauthier-Rouvière C, Bodin S, Comunale F, et al. Flotillin membrane domains in cancer. *Cancer Metastasis Rev* 2020; 39: 361-74.
42. Zhu M, Shi W, Chen K, et al. Pulsatilla saponin E suppresses viability, migration, invasion and promotes apoptosis of NSCLC cells through negatively regulating Akt/FASN pathway via inhibition of flotillin-2 in lipid raft. *J Recept Signal Transduct Res* 2022; 42: 23-33.